Epoxy Composites Reinforced by Different Size Silica Nanoparticles

Cheng-Fang Ou, Ming-Chin Shiu

Department of Chemical and Materials Engineering, National Chin-Yi University of Technology, Taichung County 411, Taiwan, Republic of China

Received 18 September 2007; accepted 25 October 2008
DOI 10.1002/app.29809
Published online 26 October 2009 in Wiley InterScience (www.interscience.wiley.com).

ABSTRACT: Three series of epoxy/SiO_2 composites, containing 0.3–7 wt % nanosized SiO_2 with different specific surface area, were prepared by solution blending. The resulting composites exhibit the higher glass transition temperature (T_g) than that of pure epoxy. The T_g of composite showed a maximum increment of 35.3°C by the addition of 7 wt % A300. The trade name of A300 is Aerosil 300. It is one of the fumed silica nanoparticles products of Degussa. The decomposition temperatures (T_d) of composites were always higher than that of pure epoxy and showed a maximum increment of 20.8°C by the addition of 5 wt % A300. The light transmittance of composites was as a function of the SiO_2 content and size. The water permeability of composites decreased with increasing SiO_2 content and the 7 wt % A300 composite exhibits a maximum decrement percentage of 35.6%. The T_g, T_d, storage modulus, and water-vapor barrier property are as a function of the SiO_2 content and size. These properties increased as the content of SiO_2 increased. The finer SiO_2 are more effective in increasing the T_g, T_d, and water-vapor barrier property. © 2009 Wiley Periodicals, Inc. J Appl Polym Sci 115: 2648–2653, 2010

Key words: epoxy; composites; morphology; transmittance; water permeability

INTRODUCTION

Epoxy resin is one of the most widely used thermosetting resins. It possesses several advantages such as low shrinkage and good chemical resistance. Therefore, epoxy resin is broadly used as adhesive, coating, casting, laminates, and encapsulation of semiconductor devices in chemical and electrical industries.[1–6] However, epoxy resins, due to their low-mechanical properties and high coefficients of thermal expansion (CTE) value compared with inorganic materials, cannot meet the requirements especially for the applications of electrical and structural such as epoxy molding compounds.[7]

The inclusion of inorganic fillers into polymers applications is primarily aimed at the cost reduction and various properties including resistance to scratching, abrasion, heat, mechanical properties,[8,9] and the barrier properties.[10] Material properties of the composites are determined by the respective properties of both physically mixed components and thus depend on the content of filler, the shape of fillers, its adhesion to polymer matrix, uniformity of dispersion, etc.[11,12] Therefore, composites with improved performance and low particle contents are highly desired.

In recent years, some studies have focused on how to improve the properties of epoxy. In many investigations,[6,7,13–15] epoxy/SiO_2 hybrid material was synthesized by the sol-gel process. Traditionally, composite materials add nanoparticles with epoxy resin to improve the property of epoxy resin. The silica particles are commonly used for the reinforcement of epoxy matrix to lower shrinkage on curing, to decrease the CTE and water/oxygen permeation, to improve thermal stability, and to meet mechanical requirements. Different metal oxide nanoparticles can be employed as filler, in particular SiO_2, TiO_2, ZnO, and CeO_2.[16,17] The silica containing nanocomposites show remarkable barrier properties to gases and moisture as well as very good resistance to staining.[18–22] Sangermano et al.[22] reported the photopolymerization of epoxy coatings containing SiO_2 nanoparticles. They found that the strong decrease on water uptake in the presence of SiO_2 makes these nanocomposites materials particularly interesting for gas-barrier coatings applications.

In this study, the epoxy/SiO_2 composites constructed by epoxy and inorganic SiO_2 nanoparticles were prepared. The thermal property, thermal stability, light transmittance, dynamic mechanical properties, and water-vapor barrier property improvement are under examination. Moreover, the effects of the SiO_2 content and size on these properties are also under investigation.

Correspondence to: C.-F. Ou (oucf@ncut.edu.tw).
Contract grant sponsor: National Science Council of the Republic of China; contract grant number: NSC95-2216-E-167-005.

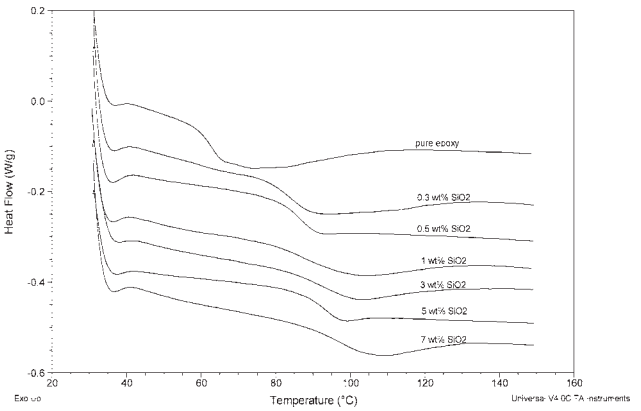

Figure 1 DSC curves of the pure epoxy and the E/A300 composites.

EXPERIMENTAL

Materials

The epoxy resin used in this study was commercial grade diglycidyl ether of bisphenol F (DGEBF; NPEL-170, epoxy equivalent weight = 160–180; Nan Ya Plastics Co., Taipei, Taiwan). The curing agent was *m*-phenylenediamines (RT30H; Epotech Composite Co., Taichung, Taiwan). Acetone was supplied by Tedia Company Inc. All chemicals were used as received. Three types of fumed silica (SiO_2) nanoparticles used for the composite preparation, was supplied by Degussa (Germany) under the trade name Aerosil 90 (A90), Aerosil 200 (A200), and Aerosil 300 (A300). The average primary particle size was 20, 12, and 7 nm and the specific surface area was 90 ± 15, 200 ± 25, and 300 ± 30 m^2/g, respectively. The SiO_2 nanopowder was dried at 70°C under vacuum for 24 h before mixing.

Preparation of composites

Epoxy was dissolved in acetone and stirred for 2 h at room temperature. After full dissolution, various SiO_2 contents 0.3, 0.5, 1, 3, 5, and 7 wt % were added into epoxy solution and then were dispersed into epoxy resin with ultrasonic instruments at 60°C for 4 h. After mixing them uniformly, 20 phr (parts per hundred resins) of curing agent were mixed into the epoxy solution. The mixtures were poured into an aluminum pan and cured at 80°C under vacuum for 24 h and then postcured at 150°C for 2 h. These samples were designed as E/A90, E/A200, and E/A300 composites. The pure epoxy (with 0% SiO_2) is prepared and cured with the same process as that of other composites.

Characterization

DSC measurements were performed with TA 2010 analyzer (TA Instruments, New Castle, DE). The sample was dried at 60°C for 6 h in a vacuum oven before DSC characterization. Appropriate amount of samples (~ 5 mg) were sealed in aluminum sample pans and heated from 30 to 200°C at a temperature scanning rate of 10°C/min under dry nitrogen atmosphere. The T_g results from the heating thermograms were the average of three samples. Thermogravimetric analyses (TGA) were performed with a TA-Q500 (TA Instruments, New Castle, DE), under a nitrogen atmosphere with a heating rate of 20°C/min from 30 to 800°C.

The morphology of the composite was obtained from scanning electron microscopic (SEM) observation using JSM-6360 (Jeol). The light transmittance analysis was measured by the UV-vis spectrometer (Jasco V-530) with wavelengths ranging from 300 to 800 nm. The water permeability of composite was determined by using Mocon Permatran-W3/61. The test was carried out at 40°C and 100% relative humidity under nitrogen atmosphere. The thicknesses of these films are about 150 μm.

Dynamic mechanical properties were determined by a dynamic mechanical analyzer (DMA) (TA-2980) between 40 and 150°C with a heating rate of 3°C/min at a frequency of 1 Hz. The rectangular bending mode was chosen and the dimension of the specimen was 40 × 7 × 0.15 mm^3.

RESULTS AND DISCUSSION

Glass transition temperature of the composites

DSC was introduced to investigate the glass transition temperature (T_g) of these composites. Figure 1 shows the DSC thermograms of E/A300 composites. It is evident that there is a distinct single T_g located at the region from 60 to 100°C in all of the samples. The DSC thermograms of another two systems E/A90 and E/A200 are similar to that of E/A300 (not shown). The T_gs were listed in Table I. The T_gs of the composites increased all the way from 62.9°C of the pure epoxy to 98.2°C in the 7 wt % A300 filled composite, implying a maximum increment by

TABLE I
Glass Transition Temperature (T_g) of Epoxy/SiO_2 Composites

	Glass transition temperature (°C)		
Composites	E/A90	E/A200	E/A300
Pure epoxy		62.9	
0.3 wt % SiO_2	72.2	81.9	83.2
0.5 wt % SiO_2	73.9	82.8	86.9
1 wt % SiO_2	77.8	85.4	87.3
3 wt % SiO_2	80.2	87.0	93.5
5 wt % SiO_2	76.8	87.2	93.8
7 wt % SiO_2	78.9	83.7	98.2

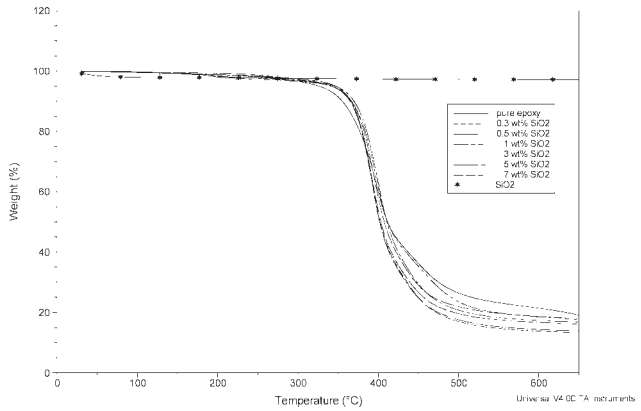

Figure 2 TGA curves of the pure epoxy and SiO_2 and the E/A300 composites.

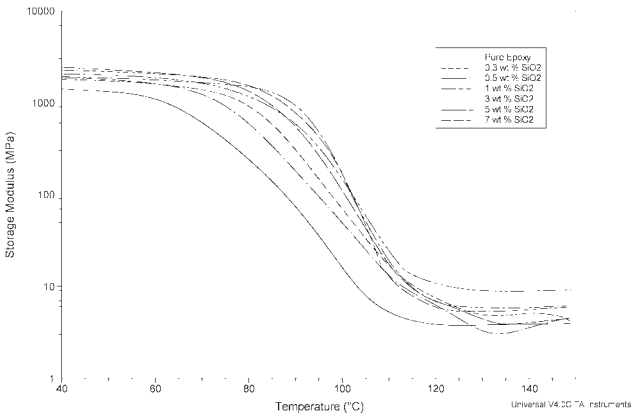

Figure 3 DMA curves of the pure epoxy and the E/A90 composites.

35.3°C. For the E/A90 and E/A200 composites systems, 3 wt % A90, 3 wt % A200 and 5 wt % A200 exhibit the highest values of T_g, respectively. The T_gs of the E/A300 composites were raised by increasing the SiO_2 content to 7 wt %. The T_gs of the E/A300 composites are always higher than those of E/A90 and E/A200 composites. These results reveal that with decreasing nanoparticle size, the T_g of composites increases. In general, the increase on T_g is attributed to a good adhesion between the polymer and reinforce particle, so that the nanometric size particle can restrict the segmental motion with a consequent increase on T_g.[23,24] At the same SiO_2 content, finer particles provides more contact area between the silica and the epoxy matrix and promotes the interfacial force between the two components to a greater degree than does the large particles.

TGA measurements

Figure 2 shows the TGA results of E/A300 composites. The data of degradation temperatures and weight percentage of residue at 650°C were listed in Table II. Pure SiO_2 does not present any abrupt decrease in weight and only a slight decrease at $\sim$ 100°C appears due to the removal of the loss of absorbed water.[25] The T_ds of the composites are always higher than that of pure epoxy (325.7°C). As for the E/A200 and E/A300, there shows a maximum at a SiO_2 content of 5 wt %, with little decrement in 7 wt % sample. The highest increment occurs in the SiO_2 compositions with 5 wt % A300; raising the T_d of epoxy from 325.7 up to 346.5°C, or an increment of 20.8°C. In comparison with the same SiO_2 content but with different sizes, the T_ds of the E/A300 composites are always higher than those of E/A90 and E/A200 composites. It seems that the finer SiO_2 could be more uniformly distributed and effective increasing the thermal stability. The result reveals that adding SiO_2 particles can improve the thermal stability of epoxy resin. In the case of composites, the weight retained after decomposition is dependent on the polymer content as shown in Table II. That is, the weight residue of composites at 650°C increases with increasing SiO_2 content.

Dynamic mechanical properties of the composites

Figure 3 shows the temperature and storage modulus of the E/A90 composites. As the temperature increases, both pure epoxy and its composites

TABLE II
The TGA Data of Epoxy/SiO_2 Composites

	T_d (°C)[a]			wt_R^{650} (%)[b]		
Composites	E/A90	E/A200	E/A300	E/A90	E/A200	E/A300
Pure epoxy		325.7			10.2	
0.3 wt % SiO_2	327.6	337.3	340.8	11.6	12.3	12.5
0.5 wt % SiO_2	334.0	337.7	341.2	13.2	13.0	13.0
1 wt % SiO_2	328.1	339.0	342.8	15.1	15.5	13.9
3 wt % SiO_2	328.8	339.5	345.9	16.4	14.3	16.5
5 wt % SiO_2	328.2	344.1	346.5	17.1	16.6	15.7
7 wt % SiO_2	328.1	338.6	341.9	22.0	22.1	17.0

[a] Degradation temperature in this table is the temperature of degradation at which the weight loss is 5%.
[b] Weight percentage of residue at 650°C.

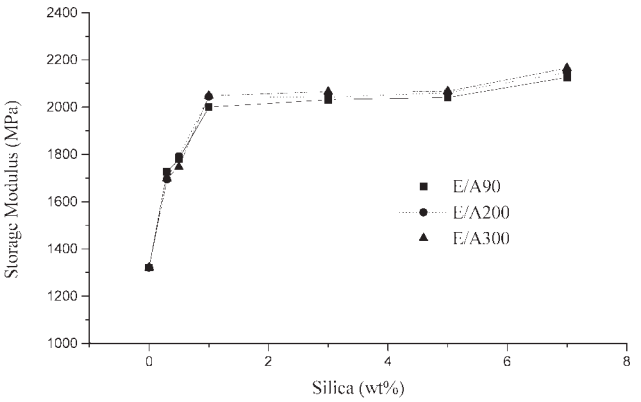

Figure 4 The storage modulus of the composites as a function of the SiO_2 content.

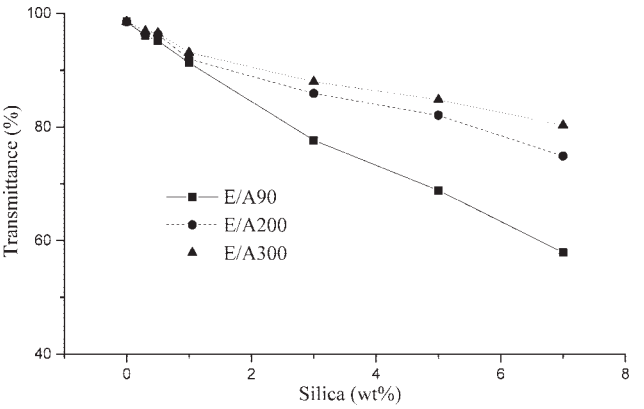

Figure 6 The light transmittance of the composites as a function of the SiO_2 content.

showed a gradual drop in storage modulus. The drop in modulus is related to the materials transition from a glassy to a rubbery state. The DMA results reconfirmed that the entire properties of composites are greatly affected by the content of fillers. The variations of the storage modulus as a function of SiO_2 content are shown in Figure 4. One can see a significant reinforcement of these composites. Storage modulus of the three system composites in glassy regions rises with increasing SiO_2 content. In comparison with the same SiO_2 contents but with different sizes, the storage modulus of the E/A300 composites is always higher than those of E/A90 and E/A200 composites. The increase in modulus can be attributed to a uniform distribution and to a good interfacial adhesion between the filler and the epoxy matrix. In fact, well dispersed nanofillers with good interactions with the polymeric matrix can improve the modulus because of the increase of constrains of the segmental motions of the polymeric chain in the composite.[26]

The light transmittance of the composites

Figure 5 shows the light transmittance of pure epoxy and E/A300 composites. The light transmittance of pure epoxy at 550 nm was as high as 98%. The spectra of 0.3 and 0.5 wt % composites show that the visible region (400–800 nm) are not affected significantly by the presence of the SiO_2 and retains the high transparency, suggesting good uniform distribution at low SiO_2 contents. The light transmittance continuously drops from the 98% of the pure epoxy to 60–83% in the 7 wt % composites, as depicted in Figure 6. The light transmittance of E/A300 composites was still higher than 80% at 550 nm as the SiO_2 content up to 7 wt %. E/A300 composites consistently exhibit higher light transmittance than those of E/A90 and E/A200, suggesting a lower degree of particle clustering. From SEM micrograph [Fig. 8(e,f)] of 7 wt % SiO_2 composites, higher agglomeration of SiO_2 dispersed in the epoxy matrix and resulted in the lower light transmittance.

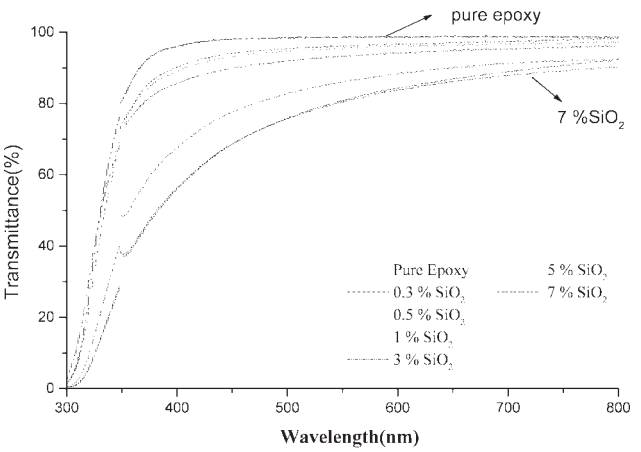

Figure 5 UV-vis spectra of the pure epoxy and the E/A300 composites.

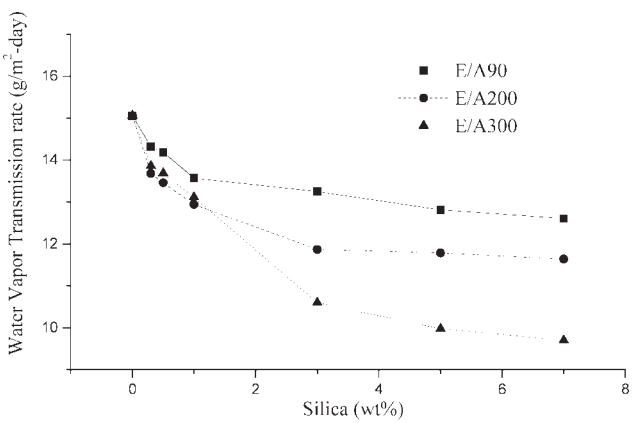

Figure 7 Water permeability of the composites as a function of the SiO_2 content.

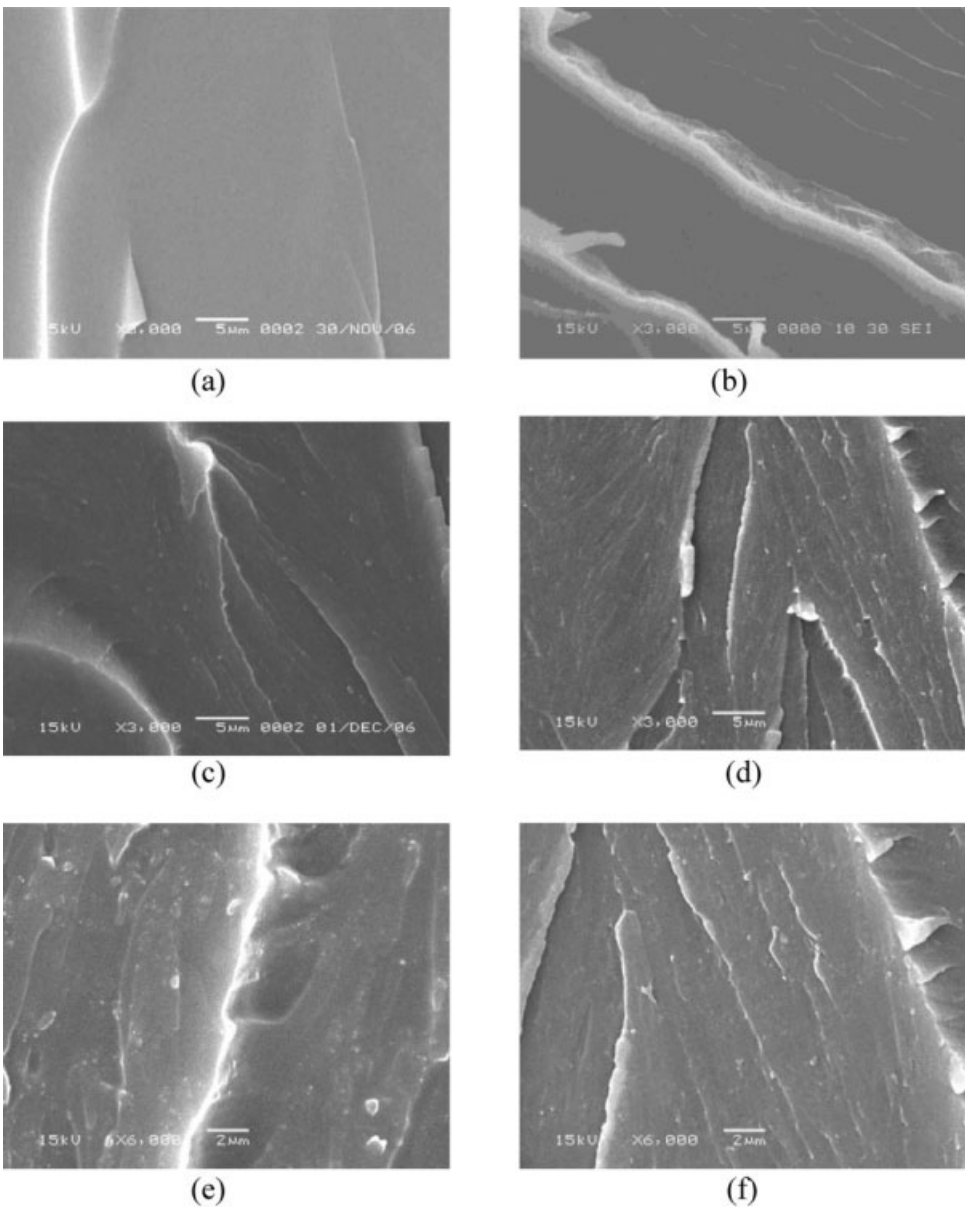

Figure 8 SEM micrographs of the fracture surfaces of samples: (a) pure epoxy; (b) 0.5 wt % A300; (c) 3 wt % A90; (d) 3 wt % A300; (e) 7 wt % A90; (f) 7 wt % A300.

Water permeability study

Figure 7 presents the SiO_2 content dependence of water permeability of the composites at 40°C. The values of water-vapor transmission rate of the samples continuously drops from the 15.06 (cc/m^2 day) of the pure epoxy to 9–13 (cc/m^2 day) in the 7 wt % composites. E/A300 composites consistently exhibit higher water-vapor barrier property (lower water-vapor transmission rate) than those of E/A90 and E/A200 composites with the same SiO_2 content. The result reveals that water-vapor barrier property of epoxy/SiO_2 improved by the addition of SiO_2 nanoparticles and increased with increasing SiO_2 content. The smaller SiO_2 increased the reinforcing effect on water-vapor barrier property. The 7 wt % A300 composite exhibits a maximum decrement by 35.6% in water permeability. The reduction of water permeability arises from the longer diffusive path that the penetrants must travel in the presence of the nanoparticle.

Morphology investigation of fractured surface

It is well known that nanoparticles would agglomerate together in the polymer matrix, and in turn decrease the reinforcing effect.[27] Figure 8 shows SEM micrographs of the fracture surface of samples. It was found that the fractured surface of pure

epoxy was very smooth and homogeneous one phase [Fig. 8(a)]. The morphology of fractured surfaces of composites with 0.5 wt % A300 [Fig. 8(b)] is the same as that of pure epoxy. It is seen that the dispersion condition of SiO_2 in the epoxy matrix are reasonably uniform in the 0.3 and 0.5 wt %. In Figure 8(c,d), the morphology of composites with 3 wt % A90 and 3 wt % A300 show the obvious change from that of pure epoxy and the agglomeration of SiO_2. The shapes of the dispersed SiO_2 droplets in 3 wt % SiO_2 composites are in spherical or elliptical geometries with the domain sizes about 0.2–0.5 μm. The number and size of dispersed droplets in 7 wt % SiO_2 composites [Fig. 8(e,f)] is more than that in 3 wt % SiO_2 composites. In other words, the agglomeration degree increases with increasing SiO_2 content. In comparison with the same SiO_2 content but with different size of A90 and A300, the composites with smaller SiO_2 show a lower agglomeration degree. This is consistent with the observation (Fig. 6) that the composites start to decrease significantly in light transmittance at 3 wt % SiO_2. Meanwhile, composites of E/A300 consistently exhibit higher light transmittance than those of E/A90 and E/A200 composites with the same SiO_2 content.

For the E/A90 and E/A200 composites systems, 3 wt % A90 and 3 wt % A200 and 5 wt % A200 exhibit the highest values of T_g, respectively. From the SEM observation, the agglomeration degree increases with increasing SiO_2 content. The 3 wt % A90, 3 wt % A200, and 5 wt % A200 composites may exhibit the most contact area between the silica and the epoxy matrix in E/A90 and E/A200 composites systems, respectively, and are most effective in increasing the T_g.

CONCLUSIONS

In this study, it was found that the epoxy/SiO_2 composites exhibited the higher T_g than that of pure epoxy and raised as the SiO_2 content increased. The T_d of the epoxy/SiO_2 composites were always higher than that of pure epoxy and showed a maximum increment of 20.8°C by the addition of 5 wt % A300. From SEM observation, 3 and 7 wt % SiO_2 composites show the agglomeration of SiO_2 and the agglomeration degree increases with increasing SiO_2 content. The light transmittance of composites decreases with increasing SiO_2 content and was still higher than 80% at 550 nm as the SiO_2 content up to 7 wt % A300. The water permeability decreased with increasing SiO_2 content and the 7 wt % A300 composite exhibits a maximum decrement percentage of 35.6%. The finer SiO_2 are more effective in increasing the T_g, T_d, and water-vapor barrier property.

References

1. Yorkgitis, E. M.; Eiss, N. S., Jr.; Tran, C.; Wilkers, G. L.; McGrath, J. E. Adv Polym Sci 1985, 72, 79.
2. Crivello, J. V.; Narayan, R. Macromolecules 1996, 29, 433.
3. Crivello, J. V. Polym Eng Sci 1992, 32, 1463.
4. Lin, S. T.; Huang, S. K. J Polym Res 1994, 1, 151.
5. Shin, S. M.; Byun, D. J.; Min, B. G.; Kim, Y. C.; Shin, D. K. Polym Bull 1995, 35, 641.
6. Weng, W. H.; Chen, H.; Tsai, S. P.; Wu, J. C. J Appl Polym Sci 2004, 91, 532.
7. Kang, S.; Hong, S. I.; Choe, C. R.; Park, M.; Rim, S.; Kim, J. Polymer 2001, 42, 879.
8. Kuo, M. C.; Huang, J. C.; Chen, M.; Jen, M. H. Mater Trans 2003, 44, 1613.
9. Cho, J. D.; Ju, H. T.; Honh, J. W. J Polym Sci: Polym Chem 2005, 43, 658.
10. Huang, C. H.; Wu, J. S.; Huang, C. C.; Lin, L. S. J Polym Res 2004, 11, 75.
11. Nielsen, L. E. Mechanical Properties of Polymers and Composites, Vol. 2; New York: Marcel Dekker, 1974.
12. Nakamura, Y.; Yamaguchi, M.; Iko, K.; Okubo, M.; Matsumoto, T. Polymer 1990, 31, 2066.
13. Hsiue, G. H.; Wang, W. J.; Chang, F. C. J Appl Polym Sci 1999, 73, 1231.
14. Chiang, C. L.; Ma, C. C. M. Eur Polym J 2002, 38, 2219.
15. Chiang, C. L.; Wang, F. Y.; Ma, C. C. M.; Chang, H. R. Polym Degrad Stab 2002, 77, 273.
16. Ou, C. F.; Hsu, M. C. J Appl Polym Sci 2007, 104, 2542.
17. Reck, E.; Seymour, S. Macromol Symp 2002, 707, 187.
18. Borup, B.; Edelmann, R.; Mehnert, R. Eur Coat J 2003, 6, 21.
19. Atsushi, B.; Toshihiko, T.; Yuichi, E.; Takashi, U. Proc Rad-Tech Sia, Yokohama, Japan, 1997; p 522.
20. Zhou, S.; Wu, L.; Sun, L. J Prog Org Coat 2002, 45, 33.
21. Bikiaris, D. N.; Vassiliou, A.; Pavlidou, E.; Karayannidis, G. P. Eur Polym J 2005, 41, 1965.
22. Sangermano, M.; Malucelli, G.; Amerio, E.; Priola, A.; Billi, E.; Rizza, G. Prog Org Coat 2005, 54, 134.
23. Chan, C. K.; Chu, I. M.; Lee, W.; Chin, W. K. Macromol Chem Phys 2001, 202, 911.
24. Ou, C. F.; Hsu, M. C. J Polym Res 2007, 14, 373.
25. Duran, A.; Serna, C.; Fornes, V.; Navarro, J. M. F. J Non-Cryst Solids 1986, 82, 69.
26. Ajayan, P. M.; Schadler, L. S.; Braun, P. V. Nanocomposite Science and Technology; Wiley: New York, 2003.
27. Kuo, M. C.; Tsai, C. M.; Huang, J. C.; Chen, M. Mater Chem Phys 2005, 90, 185.